Micro Spring Measurement and Clustering

Hsiao-Wei Liu [#1] and Yu-Yin Lan[2]

[#1,2] *Industrial Technology Research Institute, Center for Measurement Standards*
Bldg.12, No. 231, Sec. 2. Kuang Fu Rd., Hsinchu, Taiwan, R.O.C.
[#1]*rachel_liu@itri.org.tw* [2]*YuYingLan@itri.org.tw*

***Abstract*—** the pogo pins or IC probes are widely use in the semiconductor or the packaged and test industries. To fulfil the customer's demands, the design of the probe are compelled to be not only flexible but also delicate. However, one of the parts of the pogo pin is the spring whose dimension is less than 3mm in length, 0.3 mm in width, 0.03mm wire diameter. Such the "micro" spring is with the features (a) free length; (b) outer diameter; (c) active turns and (d) wire diameter. These features will influence the spring force and the yield rate as the probes manufactured. This paper aims to extract the mentioned feature by the proposed image processing techniques and cluster the diverse types of springs based on the clustering methods of (a) K-NN; (b) K-Means; (c) Max-Min and (d) Fuzzy C mean. The experiment discusses the difference among these methods.

Keywords—micro spring, measurement, clustering

1. INTRODUCTION

The springs are widely used in the every domain. The springs with the elastic characteristics can not only store the mechanical energy but also produce the force reaction. The types of springs include the compression springs, torsion springs, clips, tension springs, and clock springs [1]. The compression springs are especially used in the integrated circuit (IC) probes or pogo pins whose outer diameter and length is less than 0.5mm and 5mm, respectively. Actually, the spring force determines the displacement of a probe when these probes under testing. As a result, the features of the wire diameters, the turns and the outer diameters influence the spring force.

The springs generally are made of music wires or stainless steel wires. Based on different wire diameter of the raw materials, a spring forming machine can manufacture different compression springs. After forming the springs, these springs need to undergo the process of hot treatment to release the stress. Then the processed springs will be coated batch by batch to prevent it from the oxidization. Fig. 1 shows a spring with nine turns and its corresponding free length, outer diameter, and wire diameter.

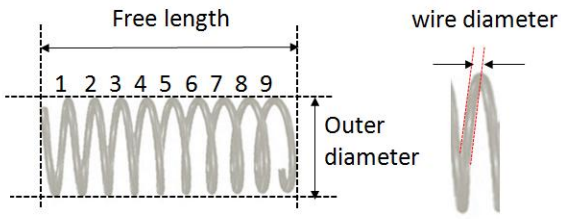

Fig. 1 The process of spring fabrication

The manufactured springs with diverse free lengths or outer diameters are chaotically packaged in a case. However, the dimensions are too tiny for human beings to recognize. Consequently, this project is to measure the spring features piece by piece to replace the human inspectors and clustering the diverse springs.

The mechanical system for capturing the spring image is shown in Fig. 2. The mechanical system is composed of the 10M mono camera, the 2X telecentric lens, and a back illumination. The field of view (F.O.V.) is approximately 3.2 *mm* in width and 2.3 *mm* in height.

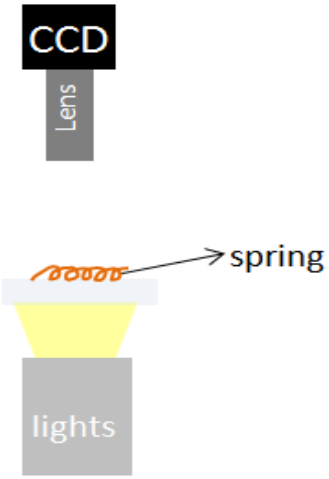

Fig. 2 The mechanical system for capturing the spring image

Four types of spring samples are chosen to evaluate this project. Table 1 lists the four type springs and its corresponding features such as active turns, outer diameter, wire diameter, and free length. Fifteen sample images of each type will be captured by the proposed mechanical system. There are totally 85 sample images. Then a sequence of image processing are executed to obtain the four feature including (a) the free length; (b) the outer diameter; (c) the wire diameter; and (d) the active turns.

Table 1. The four types of springs with its specification

Type (I)-02640 Free length:2.85±0.05mm Outer diameters: 0.17 mm Active Turns: 42 turns Wire diameters: 0.035mm	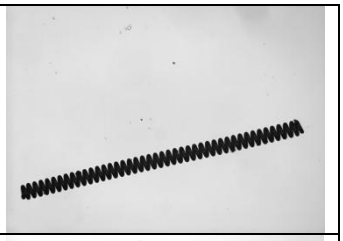
Type (II) -03123 Free length: 2.05±0.05mm Outer diameters: 0.20 mm Active Turns: 19 turns Wire diameters: 0.04mm	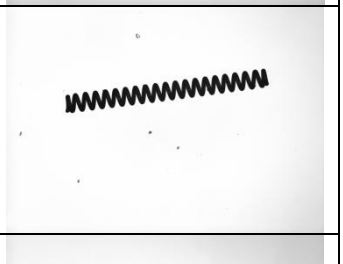
Type (III)-03524 Free length: 2.0±0.01mm Outer diameters: 0.245 mm Active Turns: 17 turns Wire diameters: 0.045mm	
Type (IV)-04039 Free length: 2.7±0.01mm Outer diameters: 0.28 mm Active Turns: 20 turns Wire diameters: 0.05mm	

2. LITERATURE REVIEWS

The common clustering method includes K-NN clustering, K-Means clustering, Max-Min clustering, Fuzzy C mean clustering. The details are as followings:

Shen et at proposed a new spatially-constrained similarity measure to address object rotation, scaling, view point change, and appearance deformation. And use the KNN re-ranking approached to have the better results [2].

James Mac Queen proposed the terminology of K-mean in 1967. Then the standard algorithm was firstly introduced by Stuart Lloyd in1957. The K-Means clustering method is a partition based algorithm [3]. Warnel and Ganorkar used K-mean clustering method to detect the disease on cotton leaves. The results was shown that K-mean clustering method using the Euclidean distance is up to 89.56% [4].

Ding et al proposed a new graph partitioning with an objective function that follows the min-max clustering principle. The algorithm of min-max cut was tested on newsgroup data sets and outperformed then other current popular clustering methods [5].

Amis et al presents a heuristic max-min d cluster in a wireless ad hoc network. The nodes were assumed to have a non-deterministic mobility pattern. The results demonstrated the heuristic is fair and stable [6].

Bezdek et al translates a programme coding of fuzzy C-Means (FCM) algorithm. Three norms, including Euclidean, Diagonal, or Mahalonobis were introduced to calculate the similarity of the feature. The adjustable weighting factor of FCM is

used to control the sensitivity noise, the acceptance of variable numbers of clusters [7]. Chaira provided a new method to compared Fuzzy c Mean by using intuitionistic fuzzy set theory apply to the medical images [8].

3. METHODOLOGY

The general recognition steps are shown in Fig. 3. The "data acquisition," "pre-processing," and "feature extraction," are executed to measure the feature of the micro spring. The diverse clustering methods, as the step of recognition or classification process, are conducted by K-NN, K-Means, Max-min, Fuzzy C mean methods. Additionally, the DYNOC measure is used as the performance index. Here, the methodology includes two phase that are micro spring measurement and micro spring clustering.

Fig. 3 Steps of the pattern recognition

3.1. Micro spring measurement

Here, the four features of the free length α, the outer diameter β, the active turn γ, and the wire diameter λ of the spring will be extracted. The 4-d features from the spring samples are as the input for the clustering procedure.

3.1.1 Image pre-processing

The image is firstly input and normalized according to the centre of the image. Figure 4(a) shows a micro spring image. Then Otsu's threshold method is applied to the Fig. 4(a). After obtaining a binary image, the connected component labelling method is used on the binary image to obtain the spring region. Figure 4(b) shows a connected component image. Based on the area, the background noise can be filter. Then the spring region can be directly obtained. Then the orientation of the selected spring region can be calculated. Based on the rotation and translation function, the spring can be normalized to the center of the image, as shown in Fig. 6(c).

3.1.2 Spring segmentation and projection

After obtaining the spring region on the normalized image, we can use the left topmost point $p_1(x_1, y_1)$ and right bottommost point $p_2(x_2, y_2)$ to generate the bonding rectangle on the spring region, as shown in Fig. 5(a). Then the contour of the spring region area calculated. Next, the row projection method on the contour executes, as shown in Fig. 5(b). After applying the projection method, the histogram can be obtained as shown in Fig. 5(c). To effectively obtain the quasi spring rectangle, the peak value (x_1' , x_2') on the two sides of the histogram is calculated. The enlarged image on the Fig. 5(c) shows two crosses that are the peak values from the histogram.

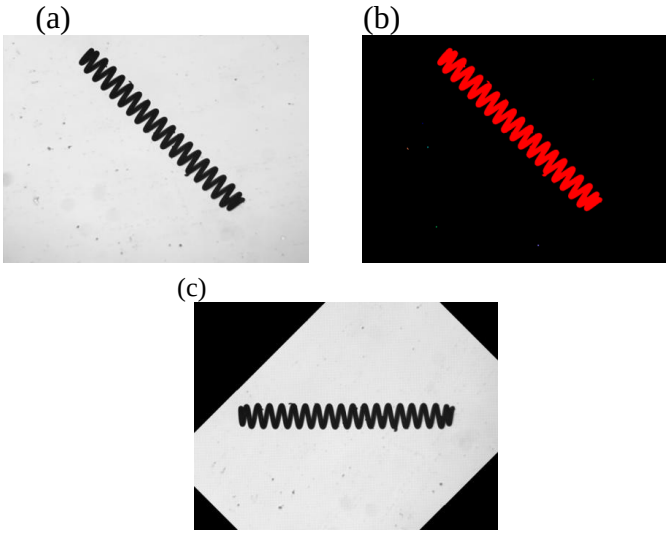

Fig. 4 (a) the original micro spring image; (b) the result using connected component method (c) the normalized image corresponding to (a)

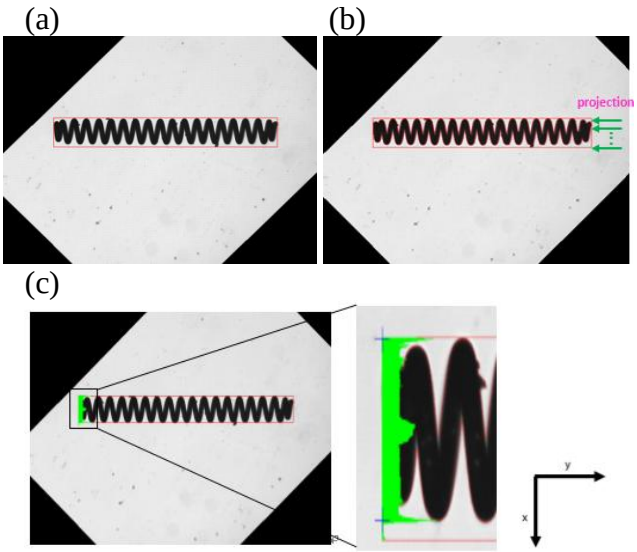

Fig. 5 (a) the bonding rectangle of the spring region; (b) projection row by row (c) the projection results and the corresponding enlarged image with the peak values

Since we obtain the coordinate of the two points of (x_1', y_1) and (x_2', y_2), then and features of free length α and outer diameter β can be calculated as below:

$$\alpha = | y_1 - y_2 | \quad (1)$$

$$\beta = | x_1' - x_2' | . \quad (2)$$

3.1.3 Region manipulation

To obtain the other features of active turn and wire diameters, the region arithmetic is adopted. Because the each turn with a summit and a valley, the crooked patterns can used to inference how many turns the spring has. To cut the crooked patterns, a cut-off range are used as value, which is one of eight multiplied by α. Figure 6(a) demonstrate the one to eight shrike rectangle (green). Figure 6(b) are the original spring contour; figure 6(c) are the intersection results between the shrink rectangle and the spring contour; figure 6(d) are the region that spring contour sub from intersected region. Then the labelling method are applied on results of figure 6(d). Each cross on the figure 6(e) are the center from the labelled regions and assume *i*-th cross on each spring. As a results, the active turns γ are calculated as

$$\gamma = \{\max(i)/2\}.$$

To effectively extract the wire diameters, three labelled regions on the two ends are dropped. Here a set of center point are selected as

$$\{ \begin{matrix} (x_i, y_i) \,|\, (x_i > x_1') and (x_i < x_2') and (i > 3) \\ and (i < \max(i) - 3) \end{matrix} \}. \quad (3)$$

Here, the *k* point are used where *k*={1,2,3,.., max(*i*)-6}. Any continues two points, e.g. (x_k, y_k) and (x_{k+1}, y_{k+1}), can generate a rectangle which can segment a piece of wire diameter. To calculate the wire diameter, the edge of the wire lines L_1 and L_2 are obtained by the wire contour. Then a midpoint p_m on the L_1 are selected to calculate the distance D_k between a point p_m and L_2, as shown in figure 7. Next, *k* sets of wire diameters are calculated and the mean wire diameter are used to yield the real wire diameter λ as

$$\lambda = \frac{1}{\max(k)} \sum_k D_k . \quad (4)$$

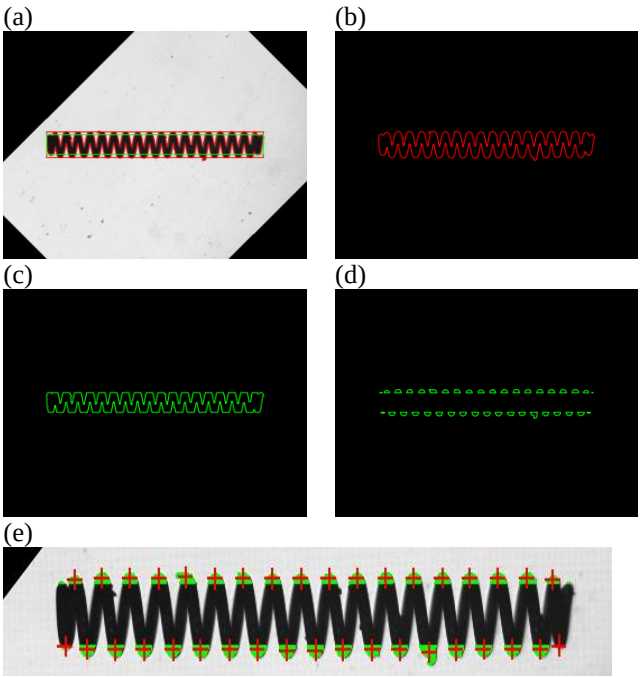

Fig. 6 (a) the shrink rectangle (green); (b) the original spring region (c) the intersection region between the shrink rectangle and the spring region; (d) projection results and the corresponding enlarged image with the peak values

(a)

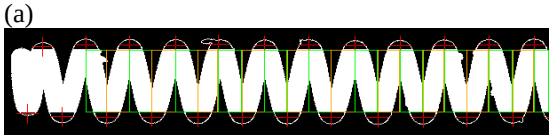

(b)

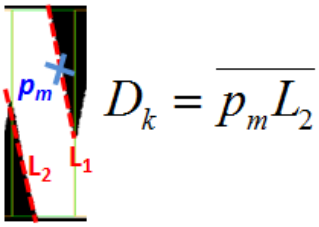

Fig. 7 (a) the segment (green or orange) rectangle by the two continues points; (b) the wire diameter calculated on D_k

4. EXPERIMENTS

The experiments are used eighty-five spring images to evaluate the K-NN, K-Means, Max-Min, and Fuzzy C clustering results. These sample images contains fifteen images of type (I) spring, twenty images of type (II) spring, thirty image of type (III) spring, and twenty images of type (IV), as listed in Table 1. Four features of free length α, outer diameter β, active turns γ, and wire diameter λ from each spring images are extracted. Each feature has different units so the experiments are under both (a) the non-normalized data points and (b) normalized data points. The normalized data point are as the normal distribution N(0,1).

Before executing the K-NN and K-Means clustering, the seeds are needed to be determined. Here, we select five seeds from the four types first. Because the four dimensions are hardly to display, the figure are used the three dimension to illustrate. Additionally, the clustering results is also based on the four dimensions. Figures 8 and 9 demonstrate the seed points, respectively.

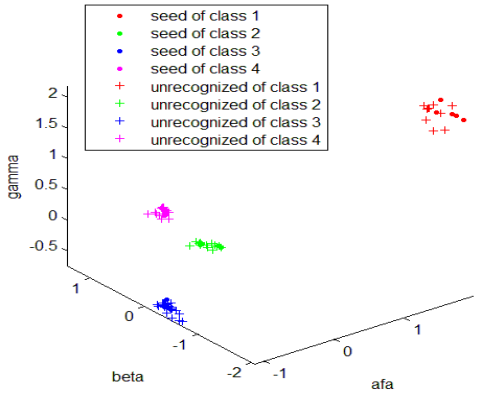

Fig. 8 Seed points from the normalized data points

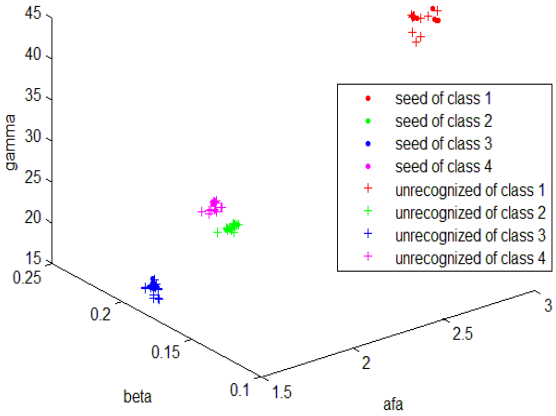

Fig. 9 Seed points from the non-normalized data points

4.1. Clustering experiments

4.1.1 K-NN clustering results

Figures 10 and 11 demonstrate the K-NN clustering results on the normalized and non-normalized data point, respectively. There are few falsely classified points on the non-normalized data point.

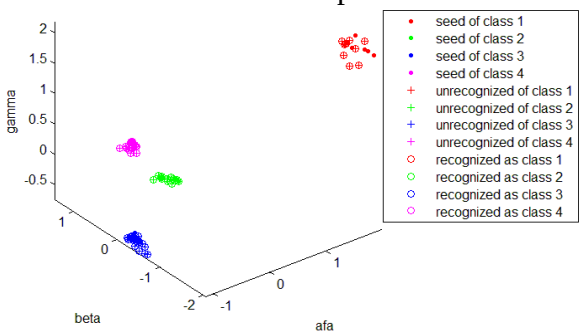

Fig. 10 KNN clustering results of the normalized data points

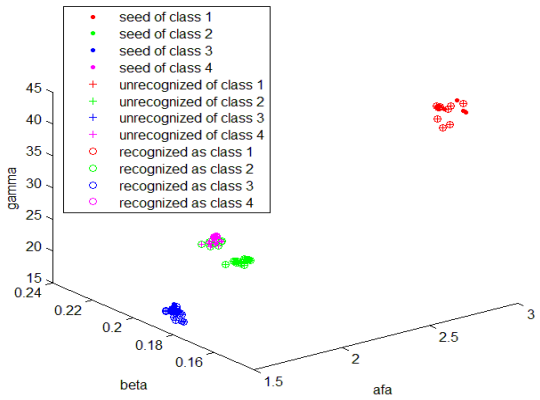

Fig. 11 KNN clustering results of the non-normalized data points

4.1.2 K-Mean clustering results

Figures 12 and 13 demonstrate the K-Means clustering results on the normalized and non-normalized data point, respectively. There are few falsely classified points on the non-normalized data point. The yellow squares are the mean point on the corresponding clusters.

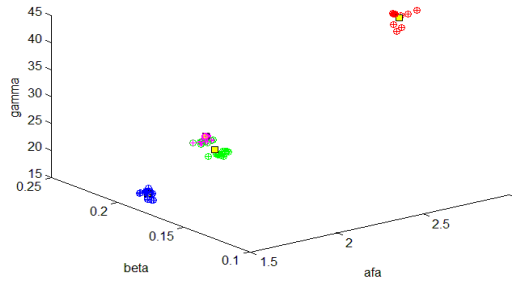

Fig. 12 K-Means clustering results of the normalized data points

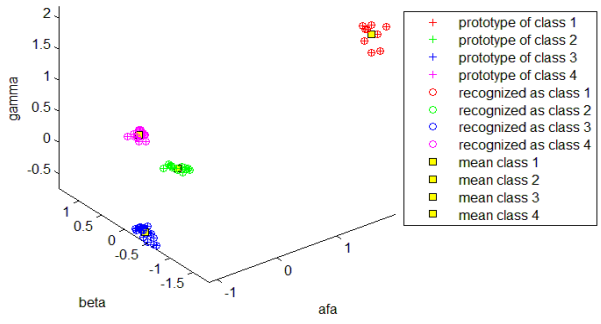

Fig. 13 K-Means clustering results of the non-normalized data points

4.1.3 Max-Min clustering results

Figures 14 and 15 demonstrate the Max-Min clustering results on the normalized and non-normalized data point, respectively. There are few falsely classified points on the non-normalized data point. The yellow squares are the mean point on the corresponding clusters; the magenta triangles are the maximum distance point between the two clusters. Here, the *t* value of the Max-Min clustering is selected as 0.3 on both the normalized and non-normalized data points. The Max-Min clustering determined how many cluster on the incoming points. As a result, the determined number of the cluster is three and four on the normalized and non-normalized data point, respectively.

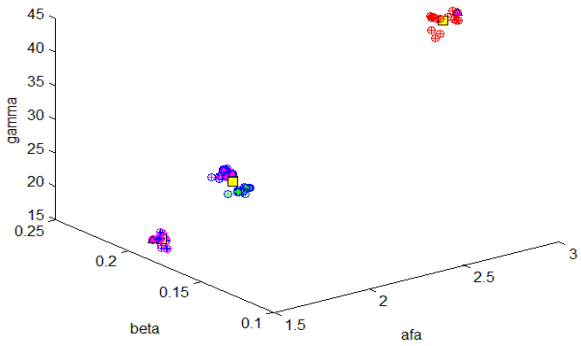

Fig. 14 Max-Min clustering results of the normalized data points

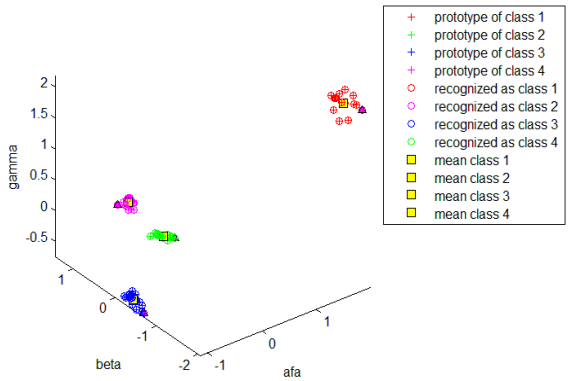

Fig. 15 Max-Min clustering results of the non-normalized data points

4.1.4 Fuzzy C Mean clustering results

Figures 16 and 17 demonstrate the Fuzzy C mean clustering results on the normalized and non-normalized data point,

respectively. The second and third classes are falsely classified into the same class on the normalized data points. Additionally, there are few points from the fourth class are classified into another cluster.

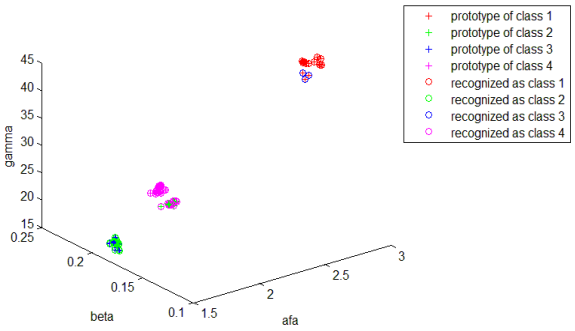

Fig. 16 Fuzzy C mean clustering results of the normalized data points

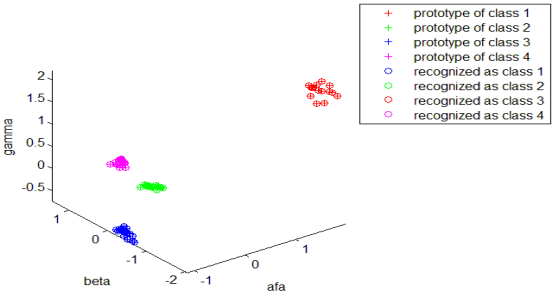

Fig. 17 Fuzzy C mean clustering results of the non-normalized data points

4.2. DYNOC measurement

Dynamic optimal cluster-seek (DYNOC) technique [9] maximizes the ratio of the minimum inter-cluster distance to the maximum intra-cluster distance.Table 1 lists the DYNOC measure on the different clustering method. Refer to the non-normalized data, the results of Fuzzy C mean has the greatest results. The Max-Min clustering results on either normalized or non-normalized data has the less difference.

Actually, the value of DYNOC is larger, the clustering result is better. The seeds of the KNN and K-Means are not included when calculating the DYNOC values. Hence, the normalized data of any clustering method are quite similar.

Table 1. The DYNOC measure versus diverse clustering methods

Methods	Normalized data		Non normalized data	
	DYNOC	Number of Cluster	DYNOC	Number of Cluster
KNN	5.5313	4	1.4723	4
K-Means	5.5313	4	1.4471	4
Max-Min	4.6291	4	3.7877	3
Fuzzy C mean	4.6291	4	55.2872	4

4.3. Classification rate

Table 2 lists the false and correct classification rate. It's observed that no false classification on the normalized data. The greatest classified results of the non-normalized data are the KNN and K-Means results. Conversely, the results of Fuzzy C mean have the worst classification.

Table 2. The classification rate

Methods	Normalized data		Non normalized data	
	False	Correct	False	Correct
KNN	0% (0/85)	100% (85/85)	5.9% (5/85)	94.1% (80/85)
K-Means	0% (0/85)	100% (85/85)	5.9% (5/85)	94.1% (80/85)
Max-Min	0% (0/85)	100% (85/85)	17.6% (15/85)	82.4% (70/85)
Fuzzy C mean	0% (0/85)	100% (85/85)	27.1% (23/85)	82.4% (70/85)

5. Conclusions

This paper has the following summaries:

1. The spring features are extracted by the proposed image processing method. The average processing time is less than 0.6 second per image.
2. Based on the 3-d distribution scatter figures, the variance between any two of clusters is smaller enough which means each cluster is far enough; as a result, the four clustering methods on the normalized data presented the almost similar results without any false classification.
3. The DYNOC values of Max-min on both normalized and non-normalized

method had the less difference. The results of Fuzzy C mean had the best performance under the non-normalized data.

4. The non-normalized data: (1) KNN and K-mean methods demonstrate the greatest results. (2) Fuzzy C Mean had the worst results.
5. The better clustering results via DYNOC measure sometimes doesn't stand for the desired results in the real word when clustering the micro springs. There is no true or false claim under such clustering results.

ACKNOWLEDGMENT

This project is under the supports of C.C.P. Contact Probes Co. Ltd., Taiwan, for providing the samples of the micro spring and the experimental equipment.

REFERENCES

[1] Springs How Products Are Made, 14 July 2007. Accessed from http://www.madehow.com/Volume-6/Springs.html

[2] X. Shen, Z. Lin, J. Brandt, S. Avidan, Y. Wu, "Object Retrieval and Localization with Spatially-Constrained Similarity Measure and K-NN Re-ranking," **2012 IEEE Conference on Computer Vision and Pattern Recognition**, pp. 3013-3020, June 2012.

[3] P. Vora, B. Oza, "A Survey on K-mean Clustering and Particle Swarm Optimization," **International Journal of Science and Modern Engineering**, vol. 1, no. 3, February 2013

[4] P. P. Warne, S. R. Ganorkar, "Detection of Diseases on Cotton Leaves Using K-Mean Clustering Method," **International Research Journal of Engineering and Technology**, vol. 2, no. 4, pp.425-431, 2015.

[5] C. H.Q. Ding, X. He, H. Zhab, M. Gu, H. D. Simon, "A Min-max Cut Algorithm for Graph Partitioning and Data Clustering," **Data Mining**, pp. 107-114, 2001.

[6] A. D. Amis, R. Prakash, T. H.P. Vuong, D. T. Huynh, "Max-Min D-Cluster Formation in Wireless Ad Hoc Networks," **the 9th Annual Joint Conference of the IEEE Computer and Communications Societies**, vol. 1, pp. 32-41, 2000.

[7] J. C. Bezdek, R. Ehrlich, W. Full, "FCM: The Fuzzy C-Means Clustering Algorithm," **Computer and Geosciences**, vol. 10, no. 2-3, pp.191-203, 1984.

[8] T. Chaira, "A Novel Intuitionistic Fuzzy C means Clustering Algorithm and Its Application to Medical Images," **Applied Soft Computing**, vol. 11, pp. 1711-1717, 2011.

[9] J. T. Tou, "DYNOC- A Dynamic Optimal Cluster-seeking Technique," **International Journal of Computer and Information Sciences**, vol. 8, no. 6, pp. 541–547, 1979